Manganese Carbonyl Nitrosyl Complexes in Solid Argon: Infrared Spectra and Density Functional Calculations

Xuefeng Wang,[†] Mingfei Zhou,[†] and Lester Andrews*

Department of Chemistry, University of Virginia, McCormick Road, P.O. Box 400319, Charlottesville, Virginia 22904-4319

Received: April 10, 2000; In Final Form: June 20, 2000

Laser-ablated manganese atoms react with CO and NO mixtures upon condensation in excess argon and further annealing to produce a series of unsaturated manganese carbonyl nitrosyl complexes including Mn(CO)(NO), $Mn(CO)(NO)_2$, and $Mn(CO)_2(NO)$. The Mn(CO)(NO) complex isomerizes to Mn(CO)(η^2-NO) on visible photolysis, which rearranges to the isocyanate OMnNCO molecule on ultraviolet photolysis. The Mn(CO)(NO)(η^2-NO) and $Mn(CO)(NO)_2$(η^2-NO) isomers also appear on annealing as does $Mn(CO)_4(NO)$. The major product after annealing is the stable 18-electron molecule $Mn(CO)(NO)_3$. The observed absorption bands of reaction products were identified by isotopic substitution ($^{13}C^{16}O$, $^{15}N^{16}O$, $^{15}N^{18}O$, and mixtures) and reproduced within 1−3% by density functional theory calculations of vibrational fundamentals. The bonding and reaction mechanisms are discussed. The isocyanate species formed here from the simple Mn(CO)(NO) complex is relevant to catalytic reactions for pollution control.

Introduction

The coordination of NO to transition metals is characterized by two different modes, e.g., end-on and side-on bonding, depending on the metal. For example, recent laser-ablation investigations of transition-metal reactions with NO in this laboratory revealed that insertion is dominant for the early metals whereas nitrosyls, both η^1 and η^2, are observed for the late metals.[1−8] Most of the metal−carbon monoxide bonding is end-on; however, photolysis of $Mn_2(CO)_{10}$ produced the bridging carbonyl mode for $Mn_2(CO)_9$.[9,10] Compared to metal carbonyls and nitrosyls, little work has been done on metal carbonyl nitrosyl complexes. The saturated stable 18-electron carbonyltrinitrosylmanganese compound ($Mn(CO)(NO)_3$) has been synthesized, its structure, spectra, and properties have been studied,[11,12] and the saturated $Mn(CO)_4(NO)$ molecule and its matrix photochemistry have also been examined.[13] The adsorption and reactions of NO and CO on Ru, Rh, and Pt surfaces have been investigated recently because of the need to remove these gases from automobile exhausts.[14,15]

In this laboratory, reactions of laser-ablated transition-metal atoms with CO,[16−22] as well as NO,[1−8] have been studied extensively. Recent laser-ablation studies of iron atom reactions with CO and NO mixtures have formed several unsaturated iron carbonyl nitrosyl complexes as reaction products,[23] and the simple Fe(CO)(NO) complex has a side-bound isomer Fe(CO)(η^2-NO). The FeCO subunit observed in different nitrosyl environments appears to distort and stiffen with an increase in positive charge on iron, which may relate to the deformability of the FeCO subunit in heme proteins. To test the general bonding and structural features of simple unsaturated transition-metal carbonyl nitrosyl complexes, we have studied the reactions of laser-ablated manganese atoms with CO and NO mixtures in excess argon during condensation at 10 K. The structures, vibrational frequencies, and infrared intensities of various manganese carbonyl nitrosyls are confirmed using isotopic substitution in the infrared spectra and density functional theory (DFT) calculations. The bonding nature of NO and CO with manganese in different carbonyl and nitrosyl environments and the photochemical rearrangement of Mn(CO)(NO) to Mn(CO)[NO] and then to the isocyanate OMnNCO are discussed.

Experimental Section

The experimental apparatus for reactions of laser-ablated metal atoms with small molecules during condensation in excess argon has been described in detail previously.[24,25] The Nd:YAG laser fundamental (1064 nm, 10 Hz repetition rate with 10 ns pulse width) was focused onto a rotating manganese target (Johnson Matthey, 99.99%). The laser energy was varied from 5 to 40 mJ/pulse. Laser-ablated metal atoms were co-deposited with nitric oxide and carbon monoxide mixtures (0.1−0.3%) in excess argon onto a 10 K CsI cryogenic window at 2−4 mmol for 1 h. Isotopic $^{15}N^{16}O$, $^{13}C^{16}O$, and $^{15}N^{18}O$ samples and mixtures were used in different experiments. Infrared spectra were recorded at 0.5 cm^{-1} resolution on Nicolet 750 with 0.1 cm^{-1} accuracy using an HgCdTe detector. Matrix samples were annealed at different temperatures, and selected samples were subjected to broadband photolysis by a medium-pressure mercury arc lamp (Philips, 175 W) with the globe removed.

Results

Infrared spectra are presented for laser-ablated manganese with NO and CO mixture, and density functional theoretical calculations of manganese carbonyl nitrosyl complexes are given for comparison.

Spectra of Reaction Products. Figures 1, 2, and 3 show the infrared spectra of laser-ablated manganese atom co-deposition with 0.2% CO + 0.2% NO in excess argon in three regions, and the absorptions are listed in Table 1. Bands due to CO, NO, $(NO)_2$, and other common N_xO_y species including N_2O,

* Author for correspondence. E-mail: lsa@virginia.edu.
[†]Permanent address: Laser Chemistry Institute, Fudan University, Shanghai, P.R.China.

10.1021/jp001370c CCC: $19.00
Published on Web 08/08/2000

TABLE 1: Infrared Absorptions (cm^{-1}) from Co-deposition of Laser-Ablated Mn Atoms with NO and CO in Argon at 10 K

CO + NO	^{13}CO + NO	CO + ^{15}NO	CO + ^{15}N^{18}O	^{12}CO/^{13}CO	^{14}NO/^{15}NO	^{15}NO/^{15}N^{18}O	assignment
2250.8	2190.7	2236.2	2237.3	1.02743	1.00653	0.9996	OMnNCO
2245.7	2185.4	2231.9	2232.7	1.02759	1.00618	0.9995	OMnNCO site
2238.2	2177.7	2225.9		1.02778	1.00553	0.9998	OMnNCO site
2230.4	2169.9	2217.4	2217.8	1.02788	1.00586		OMnNCO site
2138.2	2091.1	2138.2	2138.2	1.02252			CO
2104.6	2057.9	2104.4	2104.1	1.02269			Mn(CO)(NO)$_2$[NO]
2091.6	2045.7	2090.7	2089.6	1.02244	1.00043	1.00053	Mn(CO)(NO)$_3$
2087.0	2042.0	2087.1	2086.7	1.02204			Mn(CO)(NO)[NO]
2070.5	2026.1	2070.4	2070.4	1.02191	1.00005		late, ph dec[b]
2063.3	2017.0	2062.9	2062.8	1.02295	1.00019		Mn(CO)(NO)$_2$
2034.7	1989.2	2033.9	2033.5	1.02287			early, ph dec[b]
2028.1	1982.8	2028.1	2028.1	1.02285			Mn(CO)$_4$(NO) site
2024.1[a]	1978.8	2024.2	2024.1	1.02289			Mn(CO)$_4$(NO)
1992.8	1948.9	1992.8	1992.8	1.02255			Mn(CO)$_2$(NO), sym
1986.3	1941.9	1986.2	1986.2	1.02286			Mn(CO)$_4$(NO) site
1984.4[a]	1940.0	1984.3	1984.4	1.02289			Mn(CO)$_4$(NO)
1973.0	1924.8	1973.0	1972.9	1.02504			late[b]
1960.7	1915.3	1960.7	1960.2	1.02370			Mn(CO)[NO]
1945.7	1902.2	1944.8	1944.1	1.02287			Mn(CO)(NO)
1933.5	1891.1	1933.5	1933.0	1.02242			Mn(CO)$_2$(NO), asym
1891.1	-	1891.2	1891.0				Mn(CO)$_3$[c]
1871.8	1871.8	1839.0	1789.2		1.01784	1.02783	NO[d]
1865.1 sh	1824 sh	1865.8	1865.7	1.0225			Mn(CO)$_3$[c]
1863.2	1863.3	1830.4	1781.2		1.01792	1.02762	(NO)$_2$[d]
1832.5	1792.5	1832.5	1832.4				Mn(CO)$_2$[c]
1830.0	1829.0	1794.3[a]	1754.1	1.00055	1.01990	1.02292	Mn(CO)(NO)$_3$
1824.1	1824.1	1788.0	1747.2		1.02014	1.02335	Mn(NO)$_3$, sym[d]
1779.7	1779.7	1748.1	1702.3		1.01808	1.02690	Mn(CO)$_4$(NO)
1776.1	1776.1	1744.2	1697.5		1.01829	1.02751	(NO)$_2$[d]
1771.0	1771.0	1741.2			1.01711		Mn(CO)(NO)$_2$[NO]
1763.6	1763.6	1728.8	1690.7		1.02013	1.02254	late, ph inc[b]
1748.6	1748.6		1675.6				(MnNO)
1743.7	1743.8	1709.5[a]	1669.9		1.02001	1.02371	Mn(CO)(NO)$_3$
1728.0	1728.0	1694.1			1.02001		Mn(CO)(NO)$_2$[NO]
1722.9	1722.9	1688.4	1650.7		1.02043	1.02284	Mn(CO)$_2$(NO)
1713.2	1713.2	1679.7	1640.6	1.00023	1.01994	1.02389	Mn(NO)$_3$, asym
1708.7	1708.3	1675.1	1638.0	1.00070	1.02006	1.02265	
1704.5	1703.3	1670.9	1634.3		1.02011	1.02239	Mn(CO)(NO)
1699.8	1699.9	1665.9[a]	1628.6		1.02035	1.02290	Mn(CO)(NO)$_2$
1693.1	1693.1	1658.9[a]	1622.3		1.02062	1.02256	Mn(NO)$_2$
1504.6	1504.5	1477.8	1439.1		1.01814	1.02689	Mn(CO)(NO)$_2$[NO]
1322.1	1322.2	1299.1	1265.5		1.01770	1.02655	Mn(CO)(NO)[NO]
1298.5	1298.5	1283.5	-		1.01556	-	N$_2$O$_3$
1268.6	1268.6	1248.9[a]	1218.7		1.01577	1.02488	Mn[NO]$_2$[d]
1260.4	1260.3	1239.8	1204.4		1.01662	1.02939	site
1257.8	1257.7	1237.2	1202.1		1.01665	1.02912	Mn(CO)[NO]
1243.3	1243.3	1218.1	1199.1		1.01577	1.01585	NO$_2$-
1236.9	1236.8	1213.8	1181.0		1.01719	1.02777	Mn[NO][d]
1232.4	1232.3				1.01532		Mn[NO][d]
979.2		978.9	964.8			1.01461	X-NMnO
932.2	932.2	918.6	906.1		1.01481	1.01379	NMnO
892.3	892.3	892.3	851.0			1.04853	OMnNCO site
884.0	884.0	883.9					weak, ?
873.9	873.9	863.5	837.5		1.01204	1.03092	NMnO
867.8	867.8	867.6	825.9		1.00023	1.05049	OMnNCO
858.1	858.1	857.9	818.3			1.04839	OMnNCO site
833.3	833.3	833.2	796.7			1.04581	MnO
666.8	666.2	653.8	650.3	1.00090	1.01988	1.00538	Mn(CO)(NO)$_3$
649.6	642.7	644.6	643.6	1.01074	1.00776	1.00155	Mn(CO)$_4$(NO)
640.2	639.4	632.9	624.2	1.00125	1.01153	1.01394	Mn(CO)(NO)$_3$
631.1	629.2	622.8		1.00302	1.01333		?
542.5	542.1	529.3	523.2	1.00074	1.02494	1.01166	Mn(CO)(NO)$_3$
534.5			515.2				Mn(NO)$_3$
451.5	451.5	447.1			1.00984		Mn[NO]Mn
446.6	440.1	440.7	437.5	1.01477	1.01339	1.00731	Mn(CO)(NO)$_3$

[a] Extra bands in mixed isotopic experiments. ^{12}CO + ^{13}CO: (2024.1) 2001.7 cm^{-1}; (1984.4) 1953.2 cm^{-1}; (1832.5) 1809.0 cm^{-1}; ^{14}NO + ^{15}NO: 1820.9, 1809.8 cm^{-1} (1794.3); 1728.8, 1718.2 cm^{-1} (1709.5); 1677.1 cm^{-1} (1665.9); 1670.7 cm^{-1} (1658.9); 1353.2 cm^{-1} (1248.9). [b] Behavior of weak unassigned bands that appear on annealing. [c] Reference 22. [d] Reference 2.

NO_2, $(NO)_2^+$, NO_2^-, and $(NO)_2^-$ were also observed.[1−8] After deposition, only very weak product absorptions appeared at 1693.1 cm^{-1} (Mn(NO)$_2$), 932.2 and 873.9 cm^{-1} (NMnO), and 833.3 cm^{-1} (MnO), which are due to reaction with nitric oxide,[2] and the oxide[26] decomposition product. Stepwise annealing to 25, 30, and 35 K decreased the NMnO absorptions and produced new bands at 2091.6, 2063.3, 1945.1, 1933.5, 1830.0, 1743.7, 1713.2, and 1699.8 cm^{-1} at the expense of CO and NO at 2138.2

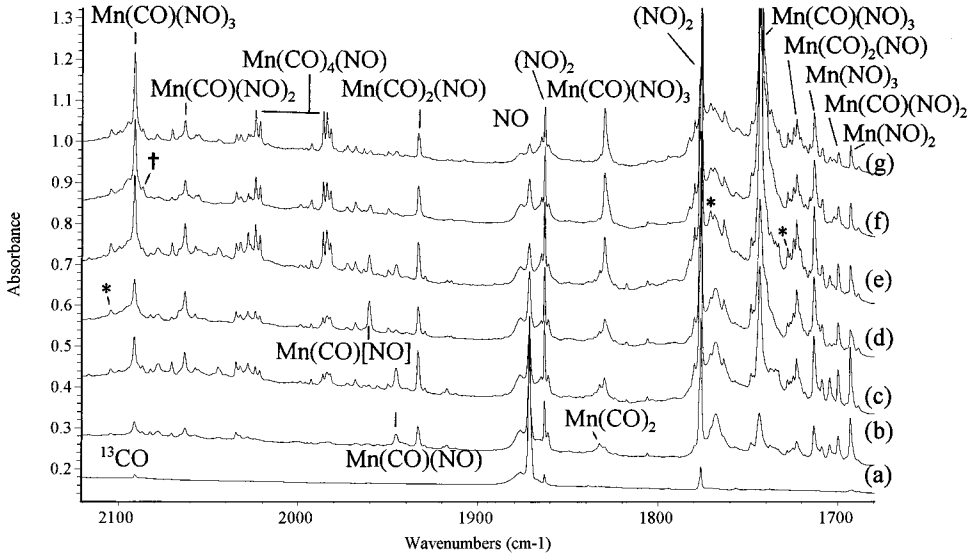

Figure 1. Infrared spectra in the 2120−1680 cm^{-1} region for laser-ablated Mn atoms co-deposited with 0.2% CO + 0.2% NO in argon at 10 K: (a) after 1 h sample deposit, (b) after annealing to 25 K, (c) after annealing to 30 K, (d) after $\lambda > 470$ nm photolysis, (e) after 35 K annealing, (f) after $\lambda > 240$ nm photolysis, and (g) after annealing to 40 K. The * denotes $Mn(CO)(NO)_2[NO]$; the † denotes Mn(CO)(NO)[NO].

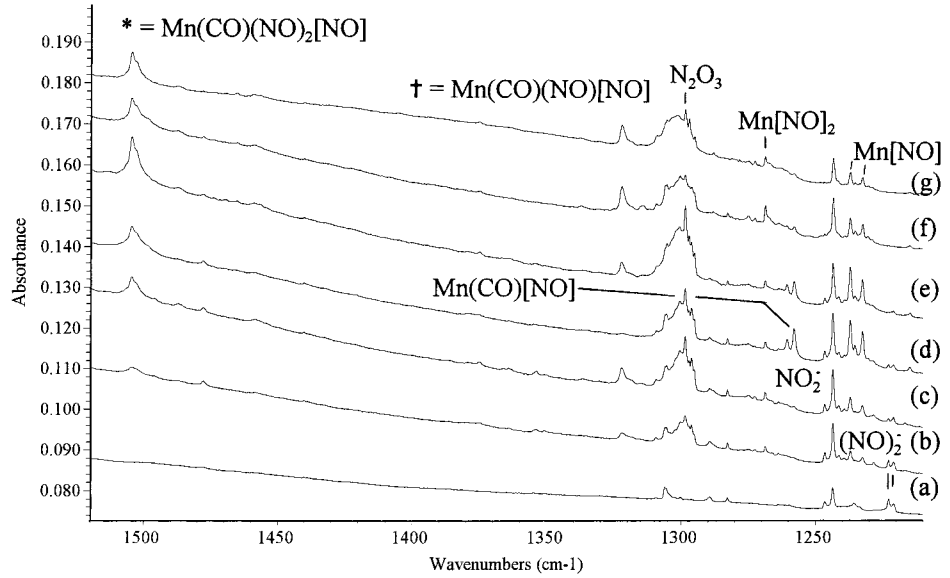

Figure 2. Infrared spectra in the 1520−1210 cm^{-1} region for laser-ablated Mn atoms co-deposited with 0.2% CO + 0.2% NO in argon at 10 K: (a) after 1 h sample deposit, (b) after annealing to 25 K, (c) after annealing to 30 K, (d) after $\lambda > 470$ nm photolysis, (e) after 35 K annealing, (f) after $\lambda > 240$ nm photolysis, and (g) after annealing to 40 K.

and 1871.8 cm^{-1}, respectively. Mercury arc photolysis using the 470 nm long-wavelength pass filter almost destroyed the 1945.1 and 1704.5 cm^{-1} absorptions, and produced new bands at 1960.7 and 1257.8 cm^{-1}; subsequent 35 K annealing reversed this change, but full arc photolysis reduced both band sets, and the original set was again increased with 40 K annealing. A final full arc photolysis decreased the 2063.3, 1960.7, 1933.5, 1713.2, and 1699.8 cm^{-1} bands, and increased the 2091.6, 1830.0, 1743.7, 666.8, and 542.5 cm^{-1} absorptions. Another band set at 2104.6, 1771.0, 1728.0, and 1504.6 cm^{-1} increased stepwise on annealing until a 30% reduction on full arc photolysis followed by recovery on 40 K annealing. Another experiment was done with 0.1% CO + 0.3% NO and the relative band populations were changed favoring the higher nitrosyl species.

Similar spectra were observed for isotopic $^{13}C^{16}O + {}^{14}N^{16}O$, $^{12}C^{16}O + {}^{15}N^{16}O$, and $^{12}C^{16}O + {}^{15}N^{18}O$ samples, and isotopic counterparts are listed in Table 1. The mixtures $^{12}C^{16}O + {}^{13}C^{16}O + {}^{14}N^{16}O$, and $^{12}C^{16}O + {}^{14}N^{16}O + {}^{15}N^{16}O$ were used for molecule identifications through isotopic shifts and splitting of product bands, and the carbonyl and nitrosyl regions are shown in Figures 4 and 5.

Calculations. The density functional method was employed in this investigation, and all calculations were carried out with GAUSSIAN 94 program.[27] The structure and frequencies of expected manganese carbonyl nitrosyls and their isomers were calculated using the BP86 functional, the 6-311+G(d) basis sets for C, N, and O atoms, and the all-electron set of Wachters and Hay as modified for manganese atoms.[28−30] The BP86 functional has been shown to give excellent frequency predictions for manganese nitrosyls and carbonyls.[2,22] All the geometrical parameters were fully optimized, and the harmonic vibrational frequencies were obtained analytically at the optimized structures. The computed geometry parameters, relative energies and frequencies, intensities, and isotopic frequency ratios for the $Mn(CO)_x(NO)_y$ ($x, y = 1, 2$) complexes are summarized in Table

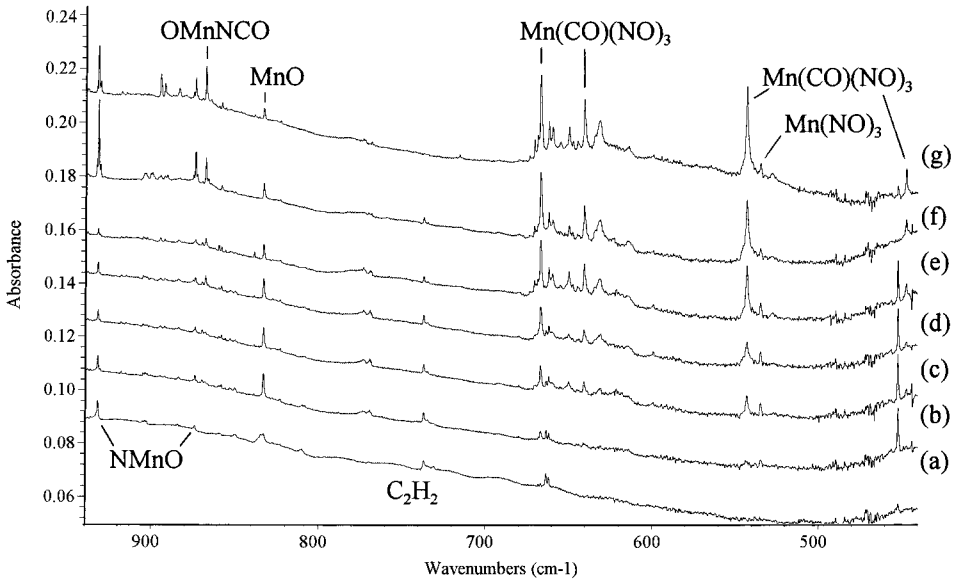

Figure 3. Infrared spectra in the 940−440 cm^{-1} region for laser-ablated Mn atoms co-deposited with 0.2% CO + 0.2% NO in argon at 10 K: (a) after 1h sample deposit, (b) after annealing to 25 K, (c) after annealing to 30 K, (d) after $\lambda > 470$ nm photolysis, (e) after 35 K annealing, (f) after $\lambda > 240$ nm photolysis, and (g) after annealing to 40 K.

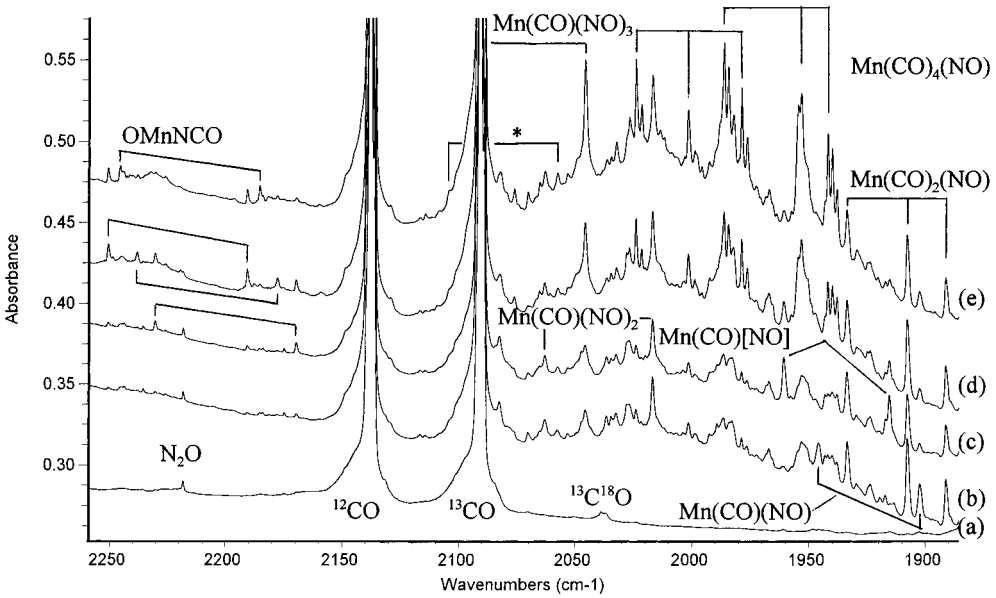

Figure 4. Infrared spectra in the 2260−1880 cm^{-1} nitrosyl region for laser-ablated Mn atoms co-deposited with 0.2% CO + 0.1% ^{14}NO + 0.1% ^{15}NO in argon at 10 K: (a) after 1 h sample deposit, (b) after annealing to 25 K, (c) after $\lambda > 470$ nm photolysis, (f) after $\lambda > 240$ nm photolysis, and (e) after annealing to 40 K.

2 and Table 3, while Table 4 contains our results for the stable 18-electron molecule, $Mn(CO)(NO)_3$. At optimized BP86/6-311+G(d) geometries, single-point energies were determined at the B3P86 level with the 6-311+G(3df) basis set.

Two isomers for carbon monoxide coordinated to manganese mononitrosyl, the end-on Mn(CO)(NO), side-on nitrosyl (Mn-CO[NO]), and two inserted oxide nitride species NMnO(CO) and OMnNCO were calculated. The first isomer is described as both ligands, CO and NO, bonding end-on with Mn, and is also known as Mn−(η^1-CO)−(η^1-NO). Two electronic states, ^{3}A′ and $^5\Sigma$ states with bent and linear structures, respectively, are very close in energy; the linear $^5\Sigma$ state is 1.3 kcal/mol higher with BP86/6-311+G(d) than the bent ^{3}A′ state, but 3.8 kcal/mol lower in energy with the B3P86/6-311+G(3df) correction. The calculated bond lengths of both Mn−C and Mn−N bonds in the linear structure are longer than those in the bent structure, while the bond lengths of CO and NO are very close to that of the free CO and NO molecules. The predicted dipole moment for bent structure is 4.136 D, much larger than that of the linear structure (0.799 D). The second isomer is Mn(CO)[NO], also known as Mn−(η^1-CO)−(η^2-NO), and three states are located with ^{3}A′ as the ground state, which is 8.1 kcal/mol higher in energy than the linear Mn(CO)(NO) molecule. (Here we use ( ) to denote η^1 and [ ] to denote η^2 coordination.) The bond length of NO in this molecule is 1.270 D, which is longer than that of free NO due to interaction with the Mn atom and suggests that Mn(CO)[NO] is the NO dissociation intermediate. For the inserted NMnO(CO) isomer, which is CO complexed to Mn in the NMnO insertion product, the ground state is ^{3}A′, which is 14.2 kcal/mol higher in energy than linear Mn(CO)(NO), and the rearranged form OMnNCO is 34.8 kcal/mol higher than Mn-(CO)(NO).

Calculations were also done for $Mn(CO)(NO)_3$, $Mn(CO)_2$-(NO), and $Mn(CO)(NO)_2$ and the results are listed in Table 2.

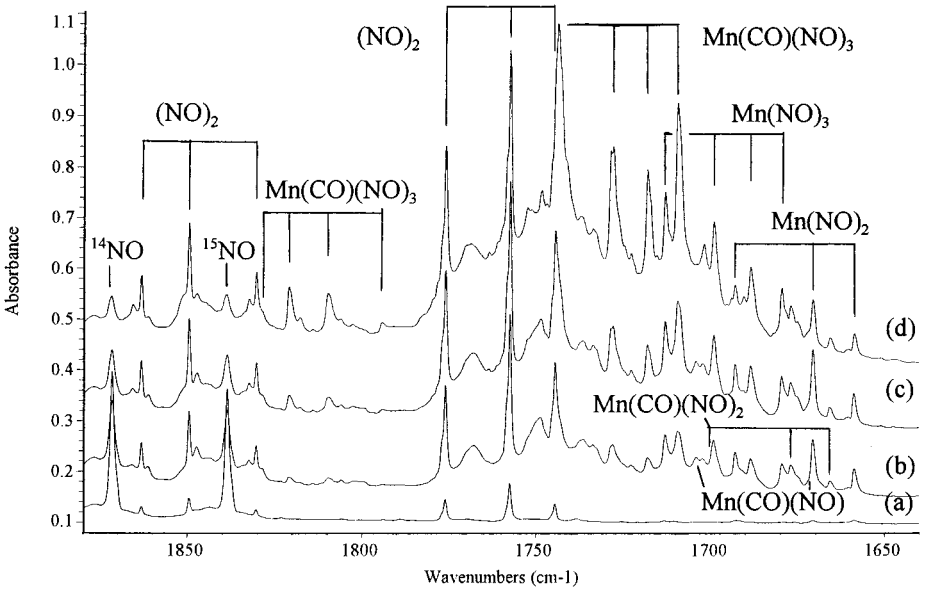

Figure 5. Infrared spectra in the 1880−1640 cm^{-1} nitrosyl region for laser-ablated Mn atoms co-deposited with 0.2% CO + 0.1% ^{14}NO + 0.1% ^{15}NO in argon at 10 K: (a) after 1 h sample deposit, (b) after annealing to 25 K, (c) after annealing to 30 K, and (d) after annealing to 35 K.

TABLE 2: States, Relative Energies (kcal/mol), and Geometries Calculated at the BP86/6-311+G(d) Level for Manganese Carbonyl Nitrosyls

molecule	state	rel energy	geometry (Å, deg)
Mn(CO)(NO)	^{3}A′	0.0 (−3.8)[a]	CO, 1.170; MnC, 1.821; NO, 1.192; MnN, 1.670; MnCO, 172.9; MnNO, 169.6; CMnN, 105.8
	$^5\Sigma$	1.3 (0.0)	CO, 1.164; MnC, 1.903; NO, 1.194; MnN, 1.727; MnCO, 180.0; MnNO, 180.0; CMnN, 180.0
Mn(CO)[NO]	^{3}A′	6.5 (8.1)	CO, 1.165; MnC, 1.871; NO, 1.270; MnN, 1.768; MnO, 1.963; MnCO, 178.2; MnNO, 78.6; OMnN, 39.4
	^{5}A′	17.4 (13.3)	CO, 1.163; MnC, 1.931; NO, 1.283; MnN, 1.824; MnO, 1.965; MnCO, 176.4; MnNO, 76.3; OMnN, 39.4
	^{7}A′	30.8 (28.8)	CO, 1.161; MnC, 1.934; NO, 1.314; MnN, 1.939; MnO, 1.950; MnCO, 177.7; MnNO, 70.8; OMnN, 39.5
NMnO(CO)	^{3}A′	−4.6 (14.2)	CO, 1.144; MnC, 1.977; MnN, 1.556; MnO, 1.615; MnCO, 180; NMnC, 120.5; OMnC, 97.5; OMnN, 142.0
	^{1}A′	17.5 (24.5)	CO, 1.156; MnC, 1.811; MnN, 1.549; MnO, 1.603; MnCO, 171.3; NMnC, 97.2; OMnC, 110.7; OMnN, 118.6
OMnNCO	$^5\Sigma$	−34.2 (34.8)	OMn, 1.601; MnN, 1.868; NC, 1.215; CO, 1.187
Mn(CO)(NO)$_2$(C_s)	^{4}A″	0.0	CO, 1.155; MnC, 1.897; NO, 1.184; MnN, 1.724; MnNO, 175.2; MnCO, 177.1; NMnN, 145.0; CMnN, 106.2
Mn(CO)(NO)[NO] (C_s)	^{4}A	12.5	CO, 1.150; MnC, 1.938; NO, 1.180; MnN, 1.711, [NO], 1.274; M[N], 1.874; Mn[O], 1.950; MnNO, MnCO, 180.0; CMnN, 115.9; CMn[N], 92.4, NMn[O], 112.9
Mn(CO)$_2$(NO) (C_s)	^{3}A″	0.0 (0.0)	CO, 1.160; NO, 1.189; MnN, 1.679; MnC, 1.873; MnCO, 177.1; NMnN, 115.5
Mn(CO)$_2$[NO]	^{3}A′	10.8 (6.4)	CO, 1.160; NO, 1.250; MnC, 1.854; MnN, 1.711; MnO, 2.092; MnCO, 180; NMnO, 36.7
Mn(CO)(NO)$_3$ (C_{3v})	$^1A_1$	0.0 (0.0)	CO, 1.154; NO, 1.172; MnC, 1.863; MnN, 1.698;
Mn(CO)(NO)$_2$[NO]	^{1}A	28.4 (25.5)	CO, 1.154; MnC, 1.848; NO, 1.175; MnN, 1.698; [NO], 1.218; Mn[N], 1.886; Mn[O], 2.052; MnNO, MnCO, 180.0; NMnN, 115.4; CMnN, 97.6; NMn[N], 120.8; NMn[O], 110.0

[a] Calculated at B3P86/6-311+G(3df,3pd) level in parentheses.

The saturated Mn(CO)(NO)$_3$ molecule was predicted to have a $^1A_1$ ground state with C_{3v} symmetry, and the calculated geometry parameters excellently reproduced the electron diffraction and microwave structure determinations.[13] The bond lengths of CO and NO are overestimated about 0.01 Å, while the lengths of MnN and MnC are underestimated about 0.02 and 0.08 Å, respectively. The predicted bond angles are much closer to experimental values; the discrepancies of NMnN and CMnN bond angles are only 0.9 and 1°, respectively. Both Mn(CO)(NO)$_2$ (^{4}A″) and Mn(CO)$_2$(NO) (^{3}A″) are calculated to have C_s symmetry. Finally, computations were also done for the Mn(CO)(NO)[NO] and Mn(CO)(NO)$_2$[NO] isomers.

Discussion

A number of manganese nitrosyls and carbonyls including Mn(CO)$_2$, Mn(CO)$_3$, MnNO, Mn(NO)$_2$, Mn(NO)$_3$, Mn[NO], Mn[NO]$_2$, and NMnO were observed in agreement with our previous investigations of the carbonyl and nitrosyl systems.[2,22] In addition, new absorptions for mixed carbonyl nitrosyls will be assigned below.

Mn(CO)(NO). The 1945.7 and 1704.5 cm^{-1} bands are produced on annealing to 25 and 30 K, but destroyed completely on visible (λ > 470 nm) and ultraviolet (λ > 240 nm) photolysis and produced again on further annealing to 35 and 40 K. The 1945.7 cm^{-1} band shows a 43.5 cm^{-1} ^{13}CO isotopic shift, but

TABLE 3: Stretching Frequencies (cm^{-1}) and Infrared Intensities (km/mol) of C−O and N−O Bonds Calculated at the BP86/6-311+G* Level for Ground States of Various Manganese Carbonyl Nitrosyls

molecule	mode	^{12}CO, ^{14}NO	^{13}CO, ^{14}NO	^{12}CO, ^{15}NO	(^{12}CO/^{13}CO)	(^{14}NO/^{15}NO)
Mn(CO)(NO) (^{3}A′)	C−O	1934.4(686)[a]	1890.4(606)	1933.5(714)	1.02327	1.00047
	N−O	1716.6(927)	1715.4(959)	1682.4(867)	1.00070	1.02033
Mn(CO)(NO) ($^5\Sigma$)	C−O	1972.6(816)	1927.9(709.1)	1971.6(865)	1.02318	1.00051
	N−O	1711.8(1271)	1710.7(1317)	1677.9(1188)	1.00064	1.02020
Mn(CO)[NO]	C−O	1973.6(746)	1927.4(705)	1973.5(747)	1.02397	1.00005
	[N−O]	1293.7(294)	1293.7(294)	1272.1(283)	1.00000	1.01698
NMnO(CO)	C−O	2085.7(602)	2037.9(568)	2085.7(602)	1.02346	1.00000
	Mn−N	1046.9(67)	1046.9(67)	1019.2(69)	1.00000	1.02718
	Mn−O	942.6(125)	942.6(125)	942.3(120)	1.00000	1.00032
OMnNCO ($^5\Sigma$)	N−C−O, a	2235.6(1409)	2173.5(1348)	2224.3(1381)	1.02857	1.00508
	N−C−O, s	1373.7(17)	1373.4(16)	1346.7(20)	1.00022	1.02005
	Mn−O	839.7(92)	839.7(92)	839.7(92)	1.00000	1.00000
Mn(CO)(NO)$_2$ (C_s)	C−O	1995.6(891)	1952.0(788.4)	1994.6(924)	1.02234	1.00050
	N−O, a	1765.7(464)	1764.4(502)	1730.7(419)	1.00074	1.02022
	N−O, s	1712.1(1713)	1712.1(1713)	1678.8(1643)	1.00000	1.01984
Mn(CO)(NO)[NO]	C−O	2040.0(709)	1994.3(645)	2039.5(727)	1.02292	1.00025
	N−O	1772.9(1056)	1772.3(1072)	1737.6(1001)	1.00034	1.02032
	[N−O]	1240.1(437)	1240.1(437)	1219.5(419)	1.00000	1.01689
Mn(CO)$_2$(NO) (C_s)	C−O, s	2013.4(365)	1968.0(308)	2012.4(395)	1.02307	1.00050
	C−O, a	1952.2(1318)	1907.5(1244)	1952.2(1319)	1.02343	1.00000
	N−O	1737.9(1071)	1736.8(1097)	1703.2(1006)	1.00063	1.02037
Mn(CO)$_2$[NO]	C−O, s	2006.9(396)	1960.5(372)	2006.9(398)	1.02367	1.00000
	C−O, a	1948.5(1386)	1903.9(1307)	1948.5(1386)	1.02343	1.00000
	N−O	1352.5(430)	1352.5(431)	1329.8(415)	1.00000	1.01707
Mn(CO)(NO)$_2$[NO]	C−O	2028.4(633)	1982.8(573)	2027.5(650)	1.02300	1.00044
	N−O, a	1804.8(606)	1803.5(624)	1769.3(579)	1.00072	1.02006
	N−O, s	1761.1(1357)	1761.1(1357)	1726.0(1301)	1.00000	1.02034
	[N−O]	1471.1(505)	1471.1(506)	1444.6(490)	1.00000	1.01834

[a] Frequency (intensity).

TABLE 4: Calculated and Observed Frequencies, Intensities, and Isotopic Frequency Ratios for Mn(CO)(NO)$_3$ ($^1A_1$) Using BP86/6-311+G*

		calcd ratios				obsd ratios			
sym	calcd freq (cm^{-1}) (km/mol)	^{12}CO/^{13}CO	^{14}NO/^{15}NO	^{15}N^{16}O/^{15}N^{18}O	obsd freq (cm^{-1}) (au)	^{12}CO/^{13}CO	^{14}NO/^{15}NO	^{15}N^{16}O/^{15}N^{18}O	assignments
e	1776.5 (1373)	1.00000	1.02045	1.02400	1743.7 (0.58)[a]	1.00000	1.02043	1.02371	NO str, asym
	679.3 (70)	1.00118	1.00876	1.01157	640.2 (0.02)	1.00125	1.01153	1.01394	MnNO, bend
	569.4 (32)	1.00035	1.02595	1.01388	542.5 (0.03)	1.00074	1.02494	1.01166	MnN str, asym
	483.1 (16)	1.01684	1.01343	1.00612	446.6 (0.01)	1.01477	1.01339	1.00731	CMnN str
	327.5 (0.1)	1.01425	1.01550	1.00750					CMnN str
	80.3 (0.0)	1.00000	1.00375	1.02564					
	69.7 (0.0)	1.00145	1.00288	1.03964					
a_1	2028.0 (614)	1.02233	1.00079	1.00059	2091.6 (0.15)	1.02244	1.00043	1.00053	CO str
	1842.0 (522)	1.00136	1.02005	1.02288	1830.0 (0.10)	1.00049	1.01990	1.02292	NO str, sym
	711.2 (95)	1.00042	1.01906	1.00461	666.8 (0.03)	1.00090	1.01988	1.00538	MnNO bend (in)
	543.3 (0.2)	1.00000	1.01551	1.02766					MnNO bend (out)
	438.8 (8)	1.01059	1.00481	1.00715					MnC s-str
	71.8 (0.2)	1.00279	1.00139	1.03763					
a_2	302.2 (0)	1.00000	1.02649	1.01343					

[a] Absorbances in Figure 1 after 40 K annealing.

only 0.9 cm^{-1} ^{15}NO and 1.6 cm^{-1} ^{15}N^{18}O isotopic shifts. This band exhibits 12/13 isotopic ratio 1.02287 and 14/15 ratio 1.00046, suggesting a terminal C−O stretching vibration with very small coupling to nitrogen. The 1704.5 cm^{-1} band shifts to 1670.9 cm^{-1} in the CO + ^{15}NO experiment (14/15 ratio 1.02035) and to 1634.3 cm^{-1} with ^{15}N^{18}O but shows only a small 1.2 cm^{-1} ^{13}CO isotopic shift. This band is due to a terminal N−O stretching mode with little carbon motion. The doublet isotopic structures for the 1945.7 and 1704.5 cm^{-1} bands observed in ^{12,13}CO + NO and CO + ^{14,15}NO experiments indicate that only one CO as well as one NO subunit are involved in the vibrational modes. These two bands are assigned to the initial unsaturated Mn(CO)(NO) complex formed in the Mn, CO, and NO reaction.

Our DFT calculations further confirm this assignment, and the results are summarized in Table 3. The calculations show that the Mn(CO)(NO) molecule has triplet bent and quintet linear structures. The energy difference between the two states is so small that it is difficult to determine which one is the ground state. The calculated C−O stretching frequency for the triplet structure is 11.3 cm^{-1} lower, but for quintet linear structure is 26.9 cm^{-1} higher than the experimental argon matrix value (1945.7 cm^{-1}), while the predicted N−O stretching frequencies for both structures are essentially the same (1716.6 and 1711.8 cm^{-1}), and much closer to the observed value (1704.5 cm^{-1}). The predicted isotopic ratios for two structures agree very well with experimental observations. The calculated relative intensities for the two structures are almost the same and in reasonable accord with the observed 0.025/0.031 band intensities. Finally, the major difference between the two structures is their dipole moments (calculated above). Our previous studies showed that the more polarizable argon matrix trends to stabilize the species

with the larger dipole moment.[17] As discussed in the following section, the frequencies of CO subunits in various manganese monocarbonyl nitrosyls modeled by BP86 are systematically lower than experimental values. So we conclude that Mn(CO)(NO) with the bent triplet state is probably observed in solid argon.

Mn(CO)[NO] or Mn(CO)(η^2-NO). The sharp bands at 1960.7 and 1257.8 cm^{-1} increase slightly on annealing to 25 and 30 K, greatly increase on $\lambda > 470$ nm photolysis, and decrease on further annealing to 35 and 40 K and $\lambda > 240$ nm photolysis, suggesting that they are due to different modes of the same molecule. The 1960.7 cm^{-1} band shifts to 1915.3 cm^{-1} in the $^{13}CO + NO$ experiment and shows a clear 1:1 doublet at 1960.7 and 1915.3 cm^{-1} in the mixed $^{12,13}CO + NO$ isotopic spectrum, indicating that only one CO subunit is involved. The 1257.8 cm^{-1} band exhibits a $^{14}NO/^{15}NO$ isotopic ratio of 1.01665, a $^{15}NO/^{15}N^{18}O$ isotopic ratio of 1.02912, and a 1:1 doublet at 1257.8 and 1237.2 cm^{-1} in the mixed $CO + ^{14,15}NO$ experiment. This band and its $^{14}NO/^{15}NO$ and $^{15}NO/^{15}N^{18}O$ isotopic ratios are much lower than the absorptions of the normal N−O stretching mode in end-on metal nitrosyls, but very close to the absorption at 1236.8 cm^{-1} and the 1.01895 $^{14}NO/^{15}NO$ and 1.02777 $^{15}NO/^{15}N^{18}O$ isotopic ratios for Mn−(η^2-NO).[1−6] These two bands are assigned to the Mn(CO)(η^2-NO) molecule.

This assignment is strongly supported by the DFT frequency calculations presented in Table 3. The stretching modes of C−O and N−O for ground $^3A'$ state Mn(CO)(η^2-NO) are predicted to be 1973.6 cm^{-1} with 1.023 97 ^{13}C isotopic ratio and 1293.7 cm^{-1} with 1.016 98 ^{15}N isotopic ratio, respectively. The deviations of isotopic ratios for each mode are only 0.03% ($^{13}CO/^{12}CO$ and $^{15}NO/^{14}NO$), indicating the calculations reproduce the experimental values extremely well.

$Mn(CO)_2(NO)$ and $Mn(CO)(NO)_2$. The 1933.5 cm^{-1} band tracks with weaker 1992.8 and 1722.9 cm^{-1} absorptions, and these three bands can be assigned to $Mn(CO)_2(NO)$. These bands increase after annealing to 20, 30, and 35 K, slightly decrease after $\lambda > 470$ nm and $\lambda > 240$ nm photolysis. The 1933.5 cm^{-1} band shifts to 1891.1 cm^{-1} in $^{13}CO + NO$ experiments with 1.022 42 $^{12}CO/^{13}CO$ isotopic ratio, and shows a 1:2:1 triplet in $^{12,13}CO + NO$ experiments. The 1973.0 cm^{-1} band likewise shifts to 1924.8 cm^{-1} with a 1.025 08 ratio. The 1722.9 cm^{-1} band shifts to 1688.4 cm^{-1} in $CO + ^{14,15}NO$ experiments with 1.019 94 $^{14}NO/^{15}NO$ isotopic ratio, and exhibits 1:1 doublet in $CO + ^{14,15}NO$ spectra. Accordingly, two carbonyl and one nitrosyl subunits are involved in this molecule.

A weak band observed at 2063.3 cm^{-1} after annealing to 20, 30, and 35 K decreases with broad band photolysis. This band tracks with a 1699.8 cm^{-1} absorption, and these two bands have very similar isotopic ratios with $Mn(CO)_2(NO)$, but 1:1 doublet $^{12,13}CO + NO$ spectra and 1:2:1 triplet $CO + ^{14,15}NO$ spectra indicate that one CO and two equivalent NO subunits are involved. These two bands are assigned to the $Mn(CO)(NO)_2$ molecule.

Similar DFT calculations were done for these two molecules, and results are listed in Tables 2 and 3. The calculations reproduced very well the observed isotopic ratios. The predicted N−O stretching modes are about 10 cm^{-1} higher than the experimental values, and the calculated C−O stretching modes are 67.7 cm^{-1} lower in the $Mn(CO)(NO)_2$ molecule, and 20.6 and 18.7 cm^{-1} higher in $Mn(CO)_2(NO)$, than the experimental observations.

Mn(CO)(NO)[NO]. A new 1322.1 cm^{-1} band increased on annealing, disappeared almost completely on $\lambda > 470$ nm photolysis, but increased on $\lambda > 240$ nm photolysis. This band showed no ^{13}CO isotopic shift, but shifted to 1299.1 cm^{-1}, and exhibited 1:1 doublet pattern in $CO + ^{14,15}NO$ spectra and shifted to 1265.5 cm^{-1} with $^{15}N^{18}O$. This band is 64.3 cm^{-1} higher than the absorption of Mn(CO)[NO] at 1257.8 cm^{-1}, and shows $^{14}NO/^{15}NO$ isotopic ratio 1.017 78, which is very close to the $^{14}NO/^{15}NO$ ratio of side-on Mn[NO].[2] The Mn(CO)(NO)[NO] molecule is proposed, and a weak CO stretching mode at 2087.0 cm^{-1} follows this unusual photolysis behavior; the associated NO mode is presumably buried in the congested 1700 cm^{-1} region.

Our DFT calculations of frequencies at 2040.0, 1772.9, and 1240.1 cm^{-1} (Table 3) support this assignment, but we again note the systematic discrepancies.

$Mn(CO)(NO)_3$. A group of prominent bands at 2091.6, 1830.0, 1743.7, 666.8, 640.2, 542.5, and 446.6 cm^{-1} can be assigned to the saturated $Mn(CO)(NO)_3$ molecule. These bands appear on deposition and increase on annealing and photolysis to become the dominant product. The absorption at 2091.6 cm^{-1} shows a 1.022 44 $^{12}CO/^{13}CO$ isotopic ratio, and although this band is overlapped by ^{13}CO absorption, a 1:1 doublet distribution is strongly suggested in $^{12,13}CO + NO$ experiments, indicating a molecule with one CO subunit. The bands at 1830.0 and 1743.7 cm^{-1} show nitrosyl stretching frequency ratios, and the mixed $CO + ^{14,15}NO$ spectra in Figure 5 show that these bands are 5.9 and 30.5 cm^{-1}, respectively, higher than the symmetric and antisymmetric stretching modes of $Mn(NO)_3$ in an argon matrix with the similar $^{14}NO/^{15}NO$ isotopic multiplets appropriate for three equivalent nitrosyl subgroups.[2] Accordingly, the 2091.6, 1830.0, and 1743.7 cm^{-1} bands are assigned to the C−O and N−O stretching modes in the $Mn(CO)(NO)_3$ molecule with C_{3v} symmetry, respectively.

The 2091.6, 1830.0, and 1743.7 cm^{-1} bands are very close to the observations of Crichton and Rest[11] for $Mn(CO)(NO)_3$ at 2091, 1829, and 1742 cm^{-1}, but there is no report of lower modes for this molecule. Four lower frequency bands at 666.8, 640.2, 542.5, and 446.6 cm^{-1} track very well with the three upper bands. The 666.8, 640.2, and 542.5 cm^{-1} bands exhibit no carbon but clear nitrogen isotopic shifts with quartet multiplets in $^{14,15}NO + CO$ experiments, and are due to Mn−N antisymmetric stretching, MnNO bending and Mn−N symmetric stretching modes. The weak band at 446.6 cm^{-1} shows both nitrogen and carbon isotopic shifts, and appears to be due to a C−Mn−N stretching mode.

The DFT calculation of frequencies and vibrational mode assignments for the $Mn(CO)(NO)_3$ molecule and the observed frequencies are summarized in Table 4. The calculation predicts very strong symmetric and antisymmetric stretching N−O modes and C−O stretching mode, as well as weak Mn−N stretching and Mn−N−O bending modes, and the calculated intensities are in very good agreement with the observed absorbances. The calculated N−O stretching modes are 12.0 and 32.8 cm^{-1} higher than the observed values, but the C−O stretching mode is underestimated by 63.6 cm^{-1}. There appears to be a systematic overestimation of N−O stretching modes but underestimation of C−O stretching modes modeled by the BP86 method for the manganese carbonyl nitrosyls. However, the predicted isotopic ratios for both N−O and C−O stretching modes are very close to the experimental results. The frequency calculation for $Mn(CO)(NO)_3$ also predicted the Mn−N stretching mode at 711.2 cm^{-1} with $^{14}NO/^{15}NO$ isotopic ratio 1.019 88 and Mn−NO bending modes at 679.3 and 569.4 cm^{-1} with $^{14}NO/^{15}NO$ isotopic ratio 1.008 76 and 1.025 95, respectively, which match well the experimental observations. The predicted 483.1 cm^{-1} band has 1.016 84 $^{12}CO/^{13}CO$ ratio and 1.013 43 $^{14}NO/^{15}NO$ ratio, which are very close to the observed C−Mn−N stretching mode at 446.6 cm^{-1} with 1.01477 and 1.01339 ratios.

$Mn(CO)(NO)_2[NO]$. The 1504.6 cm^{-1} band increased on annealing but decreased on broadband photolysis. This band

shifted to 1477.8 cm^{-1} with $^{14}NO/^{15}NO$ isotopic ratio 1.017 70, and to 1439.1 cm^{-1} with $^{15}N^{18}O$ with $^{15}NO/^{15}N^{18}O$ ratio 1.026 89, and showed 1:1 doublet pattern in CO + $^{14,15}NO$ spectra, indicating one unique NO subunit involved. This band tracks with bands at 2104.6, 1771.0, and 1728.0 cm^{-1}. These four bands agree (±1 cm^{-1}) with four bands observed on 550−640 nm photolysis of $Mn(CO)(NO)_3$ in solid argon.[11] The 2104.6 cm^{-1} band shows the appropriate $^{12}CO/^{13}CO$ ratio for a carbonyl mode. The 1771.0 and 1728.0 cm^{-1} bands are slightly higher than the symmetric and antisymmetric N−O modes for $Mn(NO)_2$ (1744.7 and 1693.0 cm^{-1}).[2] The 1504.6 cm^{-1} band is also higher than the mode for side-bound NO in Mn(CO)[NO] observed here at 1257.8 cm^{-1}. Crichton and Rest identified this molecule as $Mn(CO)(NO)_2(NO)^*$ with a different bonding arrangement for (NO)* than the conventional η^1-NO bonding.[11] We found a stable structure by DFT, 28.4 kcal/mol higher than $Mn(CO)(NO)_3$, with the diagnostic η^2-NO frequency computed slightly low at 1471.1 cm^{-1}. In addition, the other η^2-NO complexes we have characterized here support this bonding arrangement for $Mn(CO)(NO)_2[NO]$.

$Mn(CO)_4(NO)$. Weak bands produced at 2028.1, 2024.1, and 2021.6 cm^{-1} and at 1986.3, 1984.4, and 1982.2 cm^{-1} on annealing decreased slightly on each photolysis and increased more on each subsequent annealing (Figure 1). These bands reached 40% of the 2091.6 cm^{-1} carbonyl mode of $Mn(CO)(NO)_3$ on 40 K annealing. The above site split bands agree (within 1 cm^{-1}) with site split bands reported for an authentic sample of $Mn(CO)_4(NO)$ in solid argon[12] and are near the 2020 and 1996 cm^{-1} gas phase fundamentals.[31] Note that both bands formed triplet absorptions with $^{12}CO/^{13}CO$ suggesting antisymmetric C−O modes of the axial and equatorial carbonyl pairs. In addition, a very strong gas phase band at 653 cm^{-1} suggests like assignment of the 649.6 cm^{-1} band, which has the same photolysis and annealing behavior. Again, diffusion and reaction of CO and NO on annealing forms another saturated carbonyl nitrosyl.

OMnNCO. A set of weak high-frequency bands at 2250.8, 2245.7, 2238.2, and 2230.4 cm^{-1} exhibited unique photolysis and annealing behavior (Figure 4) and the 2250.8 cm^{-1} band tracked with the sharp 867.8 cm^{-1} band in the low-frequency region. The high-frequency bands show much higher $^{12}CO/^{13}CO$ ratios (1.0274−1.0278) than a normal carbonyl vibration and small $^{14}NO/^{15}NO$ ratios (1.0055−1.0061); these ratios characterize an antisymmetric carbon motion slightly involving nitrogen. Mixed ^{12}CO + ^{13}CO and ^{14}NO + ^{15}NO experiments show only isotopic doublets indicating the involvement of just one C and one N in this vibrational mode. The 867.8 cm^{-1} band shows no ^{13}CO nor ^{15}NO shift but a large $^{15}N^{18}O$ shift to 825.9 cm^{-1}, which is characteristic of a terminal Mn−O motion (867.8/825.9 = 1.050 49) (the 16/18 ratio for MnO is 1.0457).[22] Thus, the OMnNCO structure was suggested to account for this unusual vibrational motion.

Our DFT calculations predict a linear OMnNCO molecule ($^5\Sigma$) with a very strong antisymmetric N−C−O mode at 2235.6 cm^{-1} and a weak Mn−O mode at 839.7 cm^{-1}. The frequency positions match very well, but the calculated isotopic frequency ratios (1.028 57, 1.005 08) clinch the assignment. The higher frequency band has slightly less ^{13}CO shift (60.3 cm^{-1}) than calculated (62.1 cm^{-1}) but slightly more ^{15}NO shift (13.4 cm^{-1}) than computed (12.3 cm^{-1}). The lower frequency mode is calculated to have a 1.043 62 $^{16}O/^{18}O$ ratio, somewhat lower than the observed value. It is interesting to note that the $^{15}N^{18}O$ counterparts of the antisymmetric N−C−O mode show a small (~1 cm^{-1}) *blue* shift. This is due to Fermi resonance with the combination band of O−Mn and symmetric N−C−O modes, which falls in this region. Apparently the combination band is higher than the antisymmetric N−C−O mode for $^{16}OMn^{15}NCO$ but lower for $^{18}OMn^{15}NCO$ owing to the large ^{18}O−Mn isotopic shift.

TABLE 5: Summary of the Atomic Charges, MnCO Angles, and C−O Frequencies in a Series of $(NO)_xMnCO$ Molecules

				ν_{C-O} (cm^{-1})	
molecule	q_{Mn}	q_C	∠MnCO	calcd	exptl
Mn(CO) ($^6A'$)	−0.003	0.118	166.7	1951.6	1933.6[a]
Mn(NO)(CO) (^3A)	0.195	0.169	172.7	1934.4	1945.7
Mn[NO](CO) ($^3A'$)	0.136	0.241	178.2	1973.6	1960.7
$Mn(NO)_2(CO)$ ($^4A''$)	0.177	0.189	177.1	1995.6	2063.3
OMnCO ($^6\Sigma$)	0.179	0.281	180.0	2026.4	2082.5[b]
NMnO(CO) ($^3A'$)	0.234	0.311	179.9	2085.7	

[a] Reference 22, argon matrix. [b] Reference 36.

The reaction of one metal atom, CO, and NO to produce the metal isocyanate is relevant to the reaction of CO and NO on supported metal catalyst systems to remove CO and NO from auto exhausts.[14,15] These absorptions vary between 2170 and 2310 cm^{-1} depending on the support,[32−34] but the $^{12}CO/^{13}CO$ (1.0263) and $^{14}NO/^{15}NO$ (1.0044) isotopic ratios for the 2262 cm^{-1} band[32] on Cr_2O_3/Al_2O_3 are very close to the values observed here for different OMnNCO trapping sites in a solid argon matrix. It has been shown that NCO bonded to metal oxides absorbs in the 2280−2240 cm^{-1} region,[14,32−34] and the OMnNCO species observed here fits into that pattern. This work shows that one metal atom is capable of forming a complex with CO and NO, which can ultimately rearrange to the isocyanate OMnNCO (reactions 1−4 below). Clearly, the reaction with $^{15}N^{18}O$ labels the metal oxide and demonstrates that metal insertion into NO, a reduction process, is involved in the reaction mechanism.

Bonding Considerations. It is interesting to compare the Mulliken charge distributions, the MnCO bond angles, and CO stretching vibrations of MnCO subunits in the series of complexes in Table 5. For bent structures of the complexes, the MnCO bond angles and CO stretching vibrations are increased as the Mulliken charge distributions of manganese atoms become more positive. The MnCO molecule is calculated to have a sextet ground state in our recent study, which is confirmed by matrix isolation spectra in both argon and neon,[22] though MnCO was believed to have a quartet ground state from earlier DFT studies.[35] Clearly the MnCO $^6A'$ state correlates with the manganese atom with a $3d^54s^2$ configuration, which is not bound strongly to CO since there is an essentially repulsive interaction between the 5σ orbital of CO and doubly occupied 4s orbital of Mn atom. The σ repulsion is decreased if the hybridized 4s 4p$_\sigma$ polarizes away from CO,[35] and the bent structure of MnCO is obtained; however, hybrid DFT calculations find MnCO to be linear.[22] The calculated MnCO ground state is bent $^6A'$ using BP86 and linear $^6\Pi$ using B3LYP.[22] This σ repulsion is reduced in Mn−CO compounds by decreasing the electronic population in the 4s orbital through coordination of NO ligands or combination of nitrogen and oxygen atoms to the manganese center. Linear OMnCO illustrates this point.[36] As shown in Table 5, except for Mn(NO)(CO) the Mn−CO bond angles increased as charge on the center manganese becomes more positive. In addition, the π back-donation is also reduced from more positive Mn centers, and more electron-poor Mn centers produce higher CO stretching frequencies.

Reaction Mechanisms. In our previous investigations, MnCO and MnNO were not observed after matrix deposition, but they appeared on annealing;[2,22] however, the more strongly absorbing $Mn(NO)_2$ species is detected after deposition.[2] The carbonyl nitrosyl Mn(CO)(NO) is barely detected after deposition and increases on the first annealing. The more reactive MnCO and

MnNO intermediates are coordinated by NO and CO, respectively, giving Mn(CO)(NO). Reactions 1 and 2 are exothermic by 48.3 and 25.4 kcal/mol, respectively, based on B3P86/6-311+G(3df) calculated energies (BP86/6-311+G* energies give −47.7 and −14.1 kcal/mol, respectively).

$$MnCO(^6A') + NO(^2\Pi) \rightarrow Mn(CO)(NO)(^3A') \qquad \Delta E = -48.3 \text{ kcal/mol} \quad (1)$$

$$MnNO(^5A'') + CO(^1\Sigma^+) \rightarrow Mn(CO)(NO)(^3A') \qquad \Delta E = -25.4 \text{ kcal/mol} \quad (2)$$

The Mn(CO)[NO] absorption bands are produced on visible ($\lambda > 470$ nm) photolysis at the expense of Mn(CO)(NO), but destroyed by full arc ($\lambda > 240$ nm) photolysis, giving the insertion product OMnNCO, which is a higher energy species. Reactions 3 and 4 are of considerable importance in the catalytic reduction of the NO_x species to N_2 and O_2. The experiment with $^{15}N^{18}O$ shows that reduction of nitric oxide occurs to give $^{18}OMn^{15}NCO$. The NO dissociation on metal surface (Co, Ni, Rh, Ru, and Ir) have been discussed in detail.[37−41] A two-step process has been described, which appears to involve forming a dissociation side-on NO intermediate to metal center at low temperature, and then cleaving the N−O bond at higher temperature. As discussed already,[2] the insertion intermediate NMnO increases on broadband photolysis at 10 K.

$$Mn(CO)(NO)(^3A') \xrightarrow{\lambda > 470 \text{ nm}} Mn(CO)[NO](^3A') \qquad \Delta E = 8.1 \text{ kcal/mol} \quad (3)$$

$$Mn(CO)[NO](^3A') \xrightarrow{\lambda > 240 \text{ nm}} OMnNCO(^5\Sigma) \qquad \Delta E = 26.7 \text{ kcal/mol} \quad (4)$$

The unsaturated $Mn(CO)(NO)_2$ and $Mn(CO)_2(NO)$ complexes are produced on annealing. It is interesting to note that reaction 5 is less exothermic than reaction 6, although NO with one unpaired electron in a π^* orbital is more reactive than CO in most cases. It is possible that σ antibonding repulsion in $Mn(CO)(NO)_2$ from the 5σ MO of NO and the d_σ orbital of the metal center is very strong, which partly eliminates the electron pairing energy from π^* and Mn $3d_\pi$. Another $Mn(CO)(NO)_2$ isomer, involving side-on coordination of one NO, namely Mn(CO)(NO)[NO] is formed on annealing and almost destroyed by $\lambda > 470$ nm photolysis, which increases $Mn(CO)(NO)_2$ bands. Ultraviolet photolysis reverses this process.

$$Mn(CO)(NO)(^3A') + NO(^2\Pi) \rightarrow Mn(CO)(NO)_2(^4A'') \qquad \Delta E = -24.8 \text{ kcal/mol} \quad (5)$$

$$Mn(CO)(NO)(^3A') + CO(^1\Sigma^+) \rightarrow Mn(CO)_2(NO)(^3A'') \qquad \Delta E = -30.4 \text{ kcal/mol} \quad (6)$$

$$Mn(CO)(NO)_2 \underset{\lambda > 470 \text{ nm}}{\overset{\lambda > 240 \text{ nm}}{\rightleftharpoons}} Mn(CO)(NO)[NO] \quad (7)$$

The stable 18-electron $Mn(CO)(NO)_3$ molecule became the dominant product on further annealing. Note that reaction 8 is the most favorable single ligand attachment reaction observed here. We also find to appear on annealing the photochemical isomer reported by Crichton and Rest,[11] which is 28.4 kcal/mol higher than the stable $Mn(CO)(NO)_3$ isomer and involves one side bound NO ligand.

$$Mn(CO)(NO)_2(^4A'') + NO(^2\Pi) \rightarrow Mn(CO)(NO)_3(^1A_1) \qquad \Delta E = -74.7 \text{ kcal/mol} \quad (8)$$

$$Mn(CO)(NO)_2(^4A'') + NO(^2\Pi) \rightarrow Mn(CO)(NO)_2[NO] \qquad \Delta E = -46.3 \text{ kcal/mol} \quad (9)$$

Three manganese carbonyls with side-bonded NO have been observed here and the η^2-NO frequency increases from 1257.8 to 1322.1 to 1504.6 cm^{-1} on the addition of η^1-NO group(s) as less electron density is available for back-bonding to η^2-NO from the manganese center.

Although the NMnO insertion product increased 5-fold on ultraviolet photolysis in our Mn/NO experiments,[2] the side-bound Mn[NO] complex also increased in 0.4% NO experiments. However, $\lambda > 470$ nm photolysis performed here after 30 K annealing increased Mn[NO] without changing NMnO, but increased Mn(CO)[NO] and OMnNCO at the expense of Mn(CO)(NO). After 35 K annealing, Mn[NO], Mn(CO)(NO) and Mn(CO)[NO] all decreased on $\lambda > 470$ nm photolysis in favor of NMnO and OMnNCO.

Conclusions

The reactions of laser-ablated manganese atoms with CO and NO mixtures during co-deposition, and further reactions on annealing and photolysis, are investigated. The bands at 1945.7 and 1704.5 cm^{-1} increased on sample annealing and are assigned to the CO and NO stretching modes of the unsaturated Mn(CO)(NO) complex based on the ^{13}CO, ^{15}NO, and $^{15}N^{18}O$ isotopic shifts, and the spectra of isotopic mixtures. The observed spectra are reproduced within 11−12 cm^{-1} by DFT/BP86 frequency calculations. The Mn(CO)(NO) complex leads to Mn(CO)(η^2-NO) on visible photolysis, which gives the N−O insertion product isocyanate, OMnNCO, with further ultraviolet photolysis.

The $Mn(CO)(NO)_2$, Mn(CO)(NO)[NO], and $Mn(CO)_2(NO)$ complexes were also produced on annealing and identified from ^{13}CO and ^{15}NO isotopic shifts and DFT calculations. The former isomers rearrange on visible and ultraviolet photolysis. The stable 18-electron $Mn(CO)(NO)_3$ molecule becomes the dominant product on further annealing; the Mn−N, CMnN stretching, and MnNO bending modes of this molecule are reported here, as well as strong carbonyl and nitrosyl stretching modes are in agreement with early work. The side-on isomer $Mn(CO)(NO)_2$-[NO] is also formed on annealing.

In addition to Mn[NO] and $Mn[NO]_2$, mixed CO, NO samples form three manganese carbonyl nitrosyls involving side-on bonding of NO. Since the side-on arrangement can serve as a precursor for the insertion reaction that clearly leads to reduction of NO and formation of the isocyanate OMnNCO, manganese may be useful for the catalytic reduction of NO in automobile exhaust gases.

Acknowledgment. We gratefully acknowledge NSF for support of this research under grant CHE 97-00116, San Diego Supercomputer Center for computer time, and B. Liang for assistance with several experiments.

References and Notes

(1) Zhou, M. F.; Andrews, L. *J. Phys. Chem. A* **1998**, *102*, 7452 (Cr + NO).

(2) Andrews, L.; Zhou, M. F.; Ball, D. W. *J Phys. Chem. A* **1998**, *102*, 10041 (Mn, Re + NO).

(3) Andrews, L.; Zhou, M. F.; Willson, S. P.; Kushto, G. P.; Snis, A.; Panas, I. *J. Chem. Phys.* **1998**, *109*, 177 ($(NO)_2^-$).

(4) Zhou, M. F.; Andrews, L. *J. Phys. Chem. A* **1999**, *103*, 478 (V + NO); **1998**, *102*, 10025 (Nb, Ta + NO).

(5) Kushto, G. P.; Zhou, M. F.; Andrews, L.; Bauschlicher, C. W., Jr. *J. Phys. Chem. A* **1999**, *103*, 478 (Sc, Ti + NO).

(6) Andrews, L.; Zhou, M. F. *J. Phys. Chem. A* **1999**, *103*, 4167 (Mo, W + NO).

(7) Zhou, M. F.; Andrews, L. *J. Phys. Chem. A.* **2000**, *104*, 2618 (Cu + NO).
(8) Zhou, M. F.; Andrews, L. *J. Phys. Chem. A* **2000**, *104*, 3915. (Fe, Co, Ni + NO).
(9) Hepp, A. F.; Wrighton, M. S. *J. Am. Chem. Soc.* **1983**, *105*, 5934.
(10) Dunkin, I. R.; Härter, P.; Shields, C. J. *J. Am. Chem. Soc.* **1984**, *106*, 7248.
(11) Crichton, O.; Rest, A. J. *J. Chem. Soc., Dalton Trans.***1978**, 202.
(12) Rest, A. J. *J. Chem. Soc.* **1970**, 345; Crichton, O.; Rest, A. J. *J. Chem. Soc., Dalton Trans.* **1978**, 208.
(13) Hedberg, L.; Hedberg, K.; Satija, S. K.; Swanson, B. I. *Inorg. Chem.* **1985**, *24*, 2766.
(14) Kostov, K. L.; Jakob, P.; Rauscher, H.; Menzel, D. *J. Phys. Chem.* **1991**, *95*, 7785; Miners, J. H.; Bradshaw, A. M.; Gardner, P. *Phys. Chem. Chem. Phys.* **1999**, *1*, 4909.
(15) Gopinath, C. S.; Zaera, F. *J. Phys. Chem. B* **2000**, *104*, 3194. Almusaiteer, K. A.; Chuang, S. S. C. *J. Phys. Chem. B* **2000**, *104*, 2265.
(16) Zhou, M. F.; Andrews, L. *J. Am. Chem. Soc.* **1998**, *120*, 11499 (Ni + CO).
(17) Zhou, M. F.; Chertihin, G. V.; Andrews, L. *J. Chem. Phys*. **1998**, *109*, 10893; Zhou, M. F.; Andrews, L. *J. Chem. Phys*. **1999**, *110*, 10370 (Fe + CO).
(18) Zhou, M. F.; Andrews, L. *J. Phys. Chem. A* **1999**, *103*, 5259 (V, Ti + CO).
(19) Zhou, M. F.; Andrews, L. *J. Phys. Chem. A* **1999**, *103*, 6956 (Ru, Os + CO).
(20) Zhou, M. F.; Andrews, L. *J. Phys. Chem. A* **1999**, *103*, 7773 (Co, Rh, Ir + CO).
(21) Zhou, M. F.; Andrews, L. *J. Phys. Chem. A* **1999**, *103*, 7785 (Nb, Ta + CO).
(22) Andrews, L.; Zhou, M. F.; Wang, X. F.; Bauschlicher, C. W., Jr. *J. Phys. Chem. A*, in press. (Mn + CO).
(23) Wang X. F.; Zhou, M. F.; Andrews, L. *J. Phys. Chem. A* **2000**, *104*, in press.
(24) Burkholder, T. R.; Andrews, L. *J Chem. Phys*. **1991**, *95*, 8697.
(25) Hassanzadeh, P.; Andrews, L.; *J. Phys. Chem*. **1992**, *96*, 9177.
(26) Chertihin, G. V.; Andrews, L. *J. Phys. Chem. A* **1997**, *101*, 8547 (Mn + O_2).
(27) Frisch, M. J.; Trucks, G. W.; Schlegel, H. B.; Gill, P. M. W.; Johnson, B. G.; Robb, M. A.; Cheeseman, J. R.; Keith, T.; Petersson, G. A.; Montgomery, J. A.; Raghavachari, K.; Al-Laham, M. A.; Zakrzewski, V. G.; Ortiz, J. V.; Foresman, J. B.; Cioslowski, J.; Stefanov, B. B.; Nanayakkara, A.; Challacombe, M.; Peng, C. Y.; Ayala, P. Y.; Chen, W.; Wong, M. W.; Andres, J. L.; Replogle, E. S.; Gomperts, R. R.; Martin, L.; Fox, D. J.; Binkley, J. S.; Defrees, D. J.; Baker, J.; Stewart, J. P.; Head-Gordon, M.; Gonzalez, C.; Pople, J. A. *Gaussian 94*, Revision B.1; Gaussian Inc.: Pittsburgh, PA, 1995.
(28) Perdew, J. P. *Phys. Rev. B* **1986**, *33*, 8822. Becke, A. D. *J. Chem. Phys*. **1993**, *98*, 5648.
(29) McLean, A. D.; Chandler, G. S. *J. Chem. Phys*. **1980**, *72*, 5639. Krishnan, R.; Binkley, J. S.; Seeger, R.; Pople, J. A. *J. Chem. Phys*. **1980**, *72*, 650.
(30) Wachters, H. J. H. *J. Chem. Phys*. **1970**, *52*, 1033. Hay, P. J. *J. Chem. Phys*. **1977**, *66*, 4377.
(31) Barna, G.; Butler, I. S. *Can. J. Spectrosc.* **1972**, *17*, 2.
(32) Rasko, J.; Solymosi, F. *J. Chem. Soc., Faraday Trans. 1* **1980**, *76*, 2383.
(33) Lorimer, D.; Bell, A. T. *J. Catal.* **1979**, *59*, 223.
(34) Hecker, W. C.; Bell, A. T. *J. Catal*. **1984**, *85*, 389.
(35) Fournier, R.. *J. Chem. Phys*. **1993**, *98*, 8041; **1993**, *99*, 1801.
(36) Zhou, M. F.; Liang, B.; Andrews, L. *J. Phys. Chem. A* **1999**, *103*, 2013 (OMnCO).
(37) Brown, W. A.; King, D. A. *J. Phys. Chem B* **2000**, *104*, 2578, and references therein.
(38) Whitman, L. J.; Ho, W. *Surf. Sci*. **1988**, *204*, L725.
(39) Kioka, T.; Yokota, M.; Miki, H.; Sugai, S.; Kawasaki, K. *Surf. Sci.* **1989**, *216*, 409.
(40) Cornish, J. C. L.; Avery, N. R. *Surf. Sci*. **1990**, *235*, 209.
(41) Esch, F.; Baraldi, A.; Comelli, C.; Lizzit, S.; Kiskinova, M.; Cobden, P. D.; Nieuwenhuys, B. E. *J. Chem. Phys.* **1999**, *110*, 4013.